J. Pure Appl. & Ind. Phys. Vol.2 (1), 1-7 (2012)

Room Temperature Ferromagnetism of Ni Implanted SnO_2 Nanopowders

K.VADIVEL, V. ARIVAZHAGAN and S. RAJESH

Department of Physics, Karunya University, Coimbatore-641 114, India.

ABSTRACT

A novel material of $Sn_{1-x}Ni_xO_2$ nano powders were synthesized by sol-gel method. As prepared samples were characterized by X-ray Diffraction, Scanning Electron Microscopes, Photoluminescence and Elemental Dispersive X-ray analysis. By Ni-doping, not only the grain size reduces, but also the lattice volume and Intensity ratio also reduces. The crystallization becomes better with Ni concentration increasing. The EDAX analysis shows the percentage of doping. Room temperature PL signal of sample has a split in the blue green emission band. The SEM images show that the sample comprises of crystalline nanosized grains. The VSM analysis shows, the increase of concentration of Ni induce ferromagnetic property.

Keywords: Ni doped SnO_2, XRD, EDAX, SEM, PL, and VSM.

INTRODUCTION

It is of great interest in the dilute magnetic semi conductors produced by doping transition metal ions into a n-type semi conductor with a wide band gap energy rutile type SnO_2 lattice.Sno_2 has been doped separately with In, Ti, As, Sb etc to modify its properties. Recently, SnO_2 doped with 3d–transition metals has displayed some interesting semi conductivity, which may result in novel devices. In the present work, SnO_2 semi conduction has been doped with Ni to induce ferromagnetism, owing to its metal like conductivity. comparing with other preparation methods, such as PLD, MBE, sputtering and so on, sol-gel method is lower cost and easier to control the composition of DMS .In this work, we report on the structural, photoluminescence and magnetic of Ni doped SnO_2 nano powders with different Ni content from x=0.01 to 0.10 by a simple sol-gel method and obtained polycrystalline structure.

Experimental Method

The basic precursors used for the preparation of $Sn_{1-x}Ni_xO_2$, $o \leq x \leq 0.10$ nanopowders are $SnCl_4.5H_2O$ for Sn, $NiCl_2.6H_2O$ for Ni were dissolved in double distilled water. The solution was circumfluencing and an aqueous ammonia solution (1:1) was added to the above

solution drop wise. For the chemical homogeneity the dropping rate is controlled and stirring rate be controlled. Finally resulting gel was collected and washed in double distilled water. After several washing in double distilled water, the gel dried at 80°c for four hours in hot air woven. The synthesized powders were under heat treatment for 1 hour at 450°c separately. The crystalline structure of the synthesized material was analyzed by x-ray diffraction using shimadu XRD – 6000 diffractometer. The surface morphology was obtained by using JeolJsm 6390 scanning electron microscope. The photoluminescence measurements were performed by horibaJobinyvon–fluvrolog3with an applied wavelength of 365nm.The composition analysis was perform by oxford instrument – INCAPENTAFET-X3 Elemental dispersive x-ray analyzer. The magnetic property of the as prepared samples was analysized by Vibrating sample magnetometer using LAKE SHORE-7410(US).

RESULTS AND DISCUSSION

Figure (1a) shows the XRD patterns of the $Sn_{1-x}Ni_xO_2$, $0 \le x \le 0.10$ samples .XRD measurement indicate that the samples have pure rutile type tetragonal structure. The Ni doping does not impact the crystal structure of SnO_2 and also there is no trace of impurity. The full width half maximum of (110) peak decrease with Ni concentration, indicating the decrease of the crystallite size. For the tetragonal structure, the lattice parameters can be calculated from,

$$\frac{1}{d^2} = \frac{h^2 + k^2}{a^2} + \frac{l^2}{b^2} \qquad (1)$$

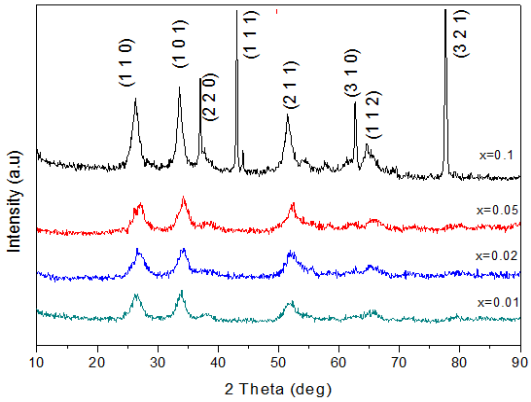

Fig (1a). XRD patterns of $Sn_{1-x}Ni_xO_2$ with (a) x=0.01 (b) x=0.02 and (c) x=0.05 (d) x=0.10

where h, k, l are all integers, 'a' and 'c' are lattice constants. The obtained Lattice constant are tabulated in table1.The 'a' and 'c' decrease with x, which could be attributed to the difference between the effective ionic radius of Ni while it is smaller than that of Sn. The little change in the Lattice constant indicates that there is a small change in Lattice volume. The intensity ratio of I(101) to I(110) decreases from 1.017 to 0.840 when the Ni concentration of Ni in the SnO_2 Lattice. The observed decrease in the intensity ratio is ascribed to the substitution of Sn by Ni in the Lattice of SnO_2.The crystalline size of the $Sn_{1-x}Ni_xO_2$, $0 \le x \le 0.10$ samples were calculated by the Debye-Scherrer's equation which is given by

$$D = \frac{k\lambda}{\beta \cos\theta} \qquad (2)$$

where 'k' is the Extinction co-efficient, ' ' is the wavelength of x-rays used, β is the full width half maximum of the peak and ɵ is the glancing angle.

Table.1. Structural parameters of $Sn_{1-x}Ni_xO_2$, as a function of Ni concentration.

Con.of Ni	h k l	FWHM (deg)	d-spacing (A°)	Grain size (nm)	Lattice Volume(A°)^3	Lattice constant	
						a(A°)	c(A°)
0.01	1 0 1 1 1 0	1.0607 1.1706	2.63991 3.34732	7.4	72.2	4.737	3.211
0.02	1 0 1 1 1 0	1.4786 1.5750	2.64898 3.34995	6.2	72.0	4.733	3.180
0.05	1 0 1 1 1 0	1.2867 1.4728	2.63141 3.32919	5.1	70.3	4.708	3.173
0.1	1 0 1 1 1 0	0.3376 0.2000	2.60493 3.22930	2.4	66.1	4.566	3.172

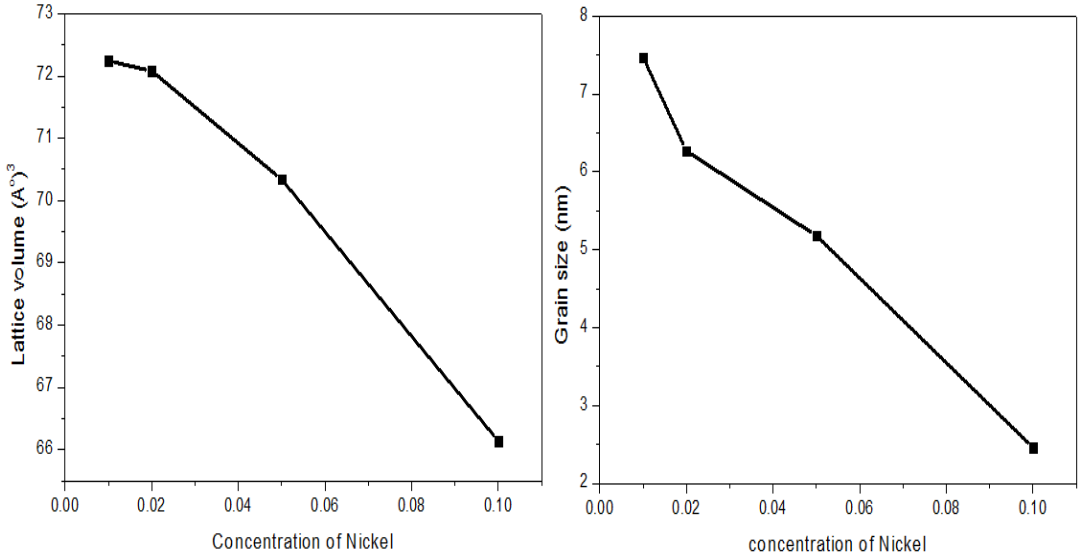

Figure (1b) Lattice volume of $Sn_{1-x}Ni_xO_2$, $0 \leq x \leq 0.10$ as a function of Ni concentration.

SEM pictures are taken for all the Sn $_{1-x}Ni_xO_2$, $0 \leq x \leq 0.10$ samples calcining for 1 hour at 450 $^{\circ}$C. All SEM pictures have been magnified to the same magnification, which is useful when comparing the sizes of the crystallites of various samples. The images show that the sample comprise of single crystalline nanosized grains. The grain size of the sample is also determined manually from the SEM micrographs. It is clearly observed that the as –prepared $Sn_{1-x}Ni_xO_2$, $0 \leq x \leq 0.10$, nanoparticles are extra fine; with an average grain size of 6nm.The result is similar to that obtained from XRD analysis.

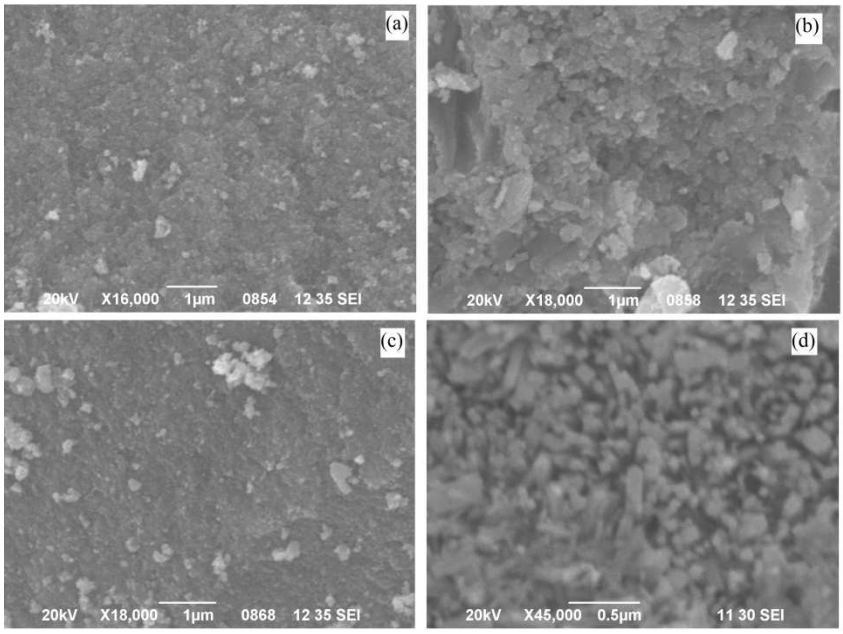

Figure (2) SEM pictures of $Sn_{1-x}Ni_xO_2$ with (a) x=0.01 (b) x=0.02 and (c) x=0.05 (d) x=0.10

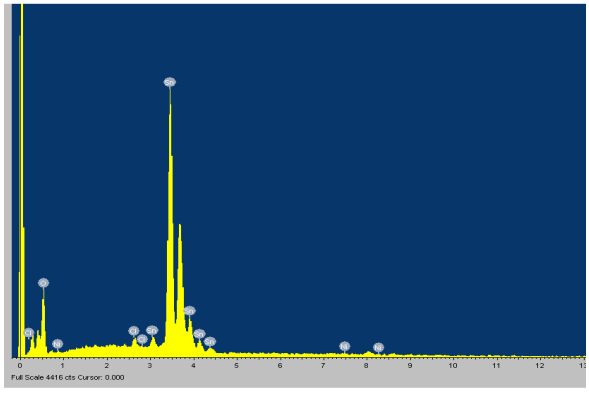

Fig (3) The EDAX spectrum of $Sn_{0.99}Ni_{0.01}O_2$

Figure (3) shows, the EDAX spectrum of $Sn_{0.99}$ $Ni_{0.01}O_2$. The EDAX spectrum shows the compositional wt% of the used materials. The weight and atomic percentage of Sn was observed as 84.19 % and 18.91 % respectively, the weight and atomic percentage of doped Ni was observed as 0.40 % and 0.18 % respectively.

Figure (4) shows the photo-luminescence spectra of samples with Ni concentration of 0.01 and 0.1 annealed at 450 °C for 1 hour. The PL spectra of the sample $Sn_{0.99}$ $Ni_{0.01}O_2$ show a broad blue green emission near 450 nm. Since the emission is lower than the band gap of pure SnO_2 (Eg=3.56eV).The spectra near 420 nm, 440 nm are split in to two peaks. From these peaks we concluded that the doping of Ni into SnO_2.

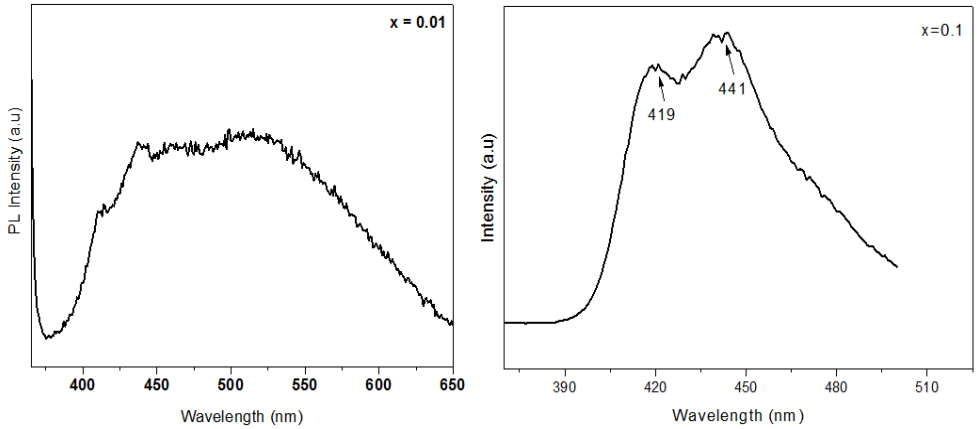

Figure (2) Room temperature PL spectra of SnO2 with Ni concentrations of 0.01 and 0.1

Figure (5) shows the VSM hysteresis loops for Sn_{1-x} Ni_xO_2,$0 \leq X \leq 0.10$ Nano powders on at room temperature. From the hysteresis loops of x=0.01,0.02 and 0.05 shown to be of diamagnetic behavior. Further increasing the Ni concentration x=0.10, we get the ferromagnetic behavior of the sample. The magnetic moment of the sample is 25.05memu/g. The Coercivity of the sample is 47.011µemu. Now, before ascribing the observed room-temperature ferromagnetism to be intrinsic in our case, one should rule out the possibility that the impurity phase is responsible for ferromagnetism, although no secondary phase was observed in the XRD pattern. Since no additional phases such as Ni clusters and NiO were seen in the sample. Thus, the Ni-related secondary phases cannot be responsible for the ferromagnetic behavior in our case. Hence, the observed ferromagnetism could be due to the incorporation of Ni ions into the Sno_2. Lattice and has an intrinsic origin. Much of the magnetic moment however is associated with electronic defects or lattice defects. The

dopants somehow serve to activate the defect moment, since the undoped Sno_2 are not ferromagnetic. The doping of magnetic Ni icons could introduce defects into Sno_2 lattice and thus long-range magnetic ordering in grains could be interrupted.

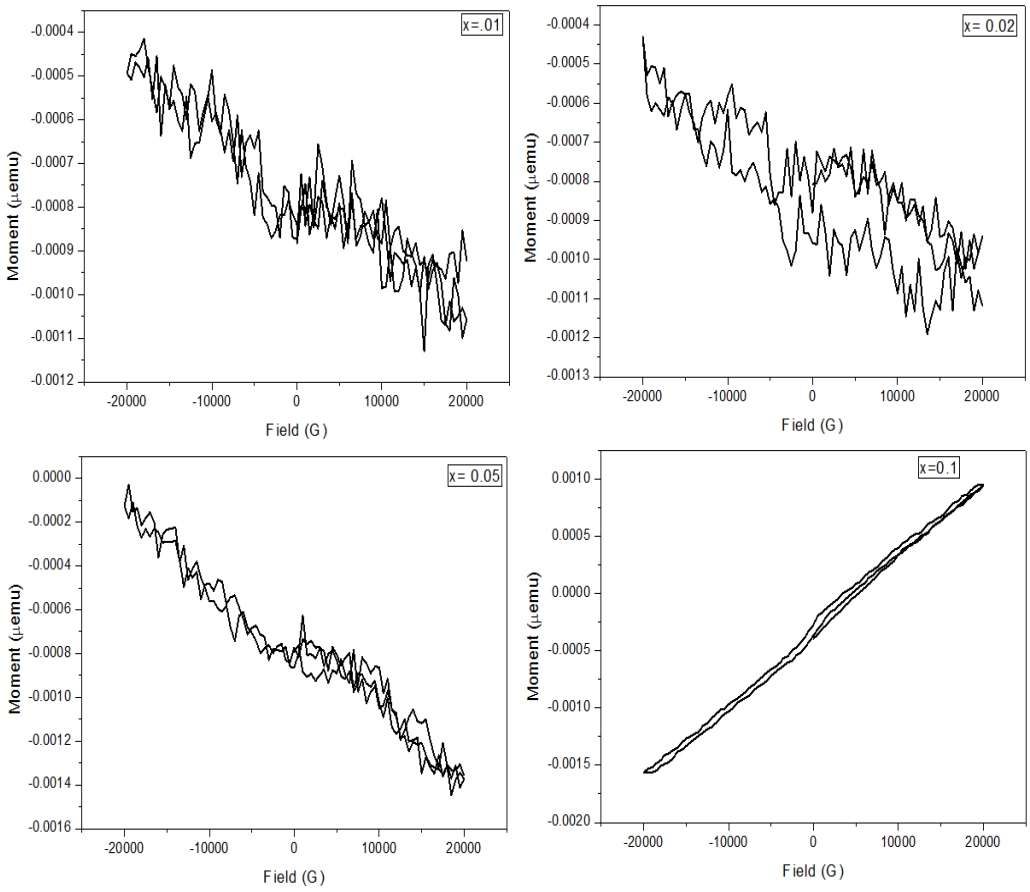

Fig.5. VSM plot of $Sn1_{-x}Ni_xO_2$ with different Ni concentrations

This results in relatively weak coupling between the sub-lattices and gives rise to ferromagnetism by double exchange through the introduced magnetic Ni ions and free charge carriers. Thus Ni doping in Sno_2 seems to offer a great deal of interest as a potential candidate for spintronics because of its RTFM behavior. This behavior can be understood as the Ni concentration plays an important role in producing ferromagnetic property in Sn_{1-x} Ni_xO_2 $_{Nano}$ powders.

CONCLUSION

SnO_2: Ni Nano Powders have been prepared by sol-gel method.XRD

measurements indicate that the grain size decrease and the lattice volume decrease with nickel content increasing. The PL spectrum consist of a strong UV peak, but it is not clear and a broad blue green peak. The EDAX spectrum confirm the doping composition and SEM images show that samples comprise of crystalline nanosized grains. A systematic change in magnetic behavior from diamagnetic to ferromagnetic was observed with increase in doping composition from x=0.01 to x=0.10 has been observed in Sn_{1-x} Ni_xo_2, x=0.01 to x=0.10 Nanopowders synthesized at 450°C. The present study reveals a strong magneto-structural correlation in Sn_{1-x} Ni_xO_2 Nanopowders and its dependence of Ni doping composition. Thus Ni concentration plays an important role in inducing the ferromagnetism in Sn_{1-x} Ni_xO_2 Nanopowders.

ACKNOWLEDGEMENT

Author's would like to thank SAIF, IIT, Chennai, Tamilnadu, India.

REFERENCES

1. K. Vadivel, V. Arivazhagan, S. Rajesh *IJSER*, 2, 4, (2011).
2. R. S. Rusu, G. I. Russia, *J. Optoelectron. Adv. Mater* 7(2), 823 (2005).
3. M. Penza, S. Cozzi, M. A. Tagliente, A. Quirini, *Thin Solid Films*, 71, 349 (1999).
4. S. Ishibashi, Y. Higuchi, K. Nakamura, *J. Vac. Sci. Technol*., A8, 1403 (1998).
5. J. Joseph, V, K. E. Abraham, Chinese *Journal of Physics*, 45, No.1, 84 (2007).
6. E. Elangovan, K. Ramamurthi, *Cryst. Res. Technol.*, 38(9), 779 (2003).
7. Datazoglov O. *Thin Solid Films*, Vol. 302, 204-213, (1997).
8. Badawy W.A et al *Electrochem, Soc*., Vol.137, 1592-1595,(1990).
9. Bruneaux J. *et al*, *Thin Solid Films*, Vol.197, 129-142, (1991).
10. Chitra Agashe *et al*. *J. Appl. Phys*. Vol.70, 7382-7386, (1991).
11. Datazoglov O. *Thin Solid Films*, Vol.302, 204-213,(1997)
12. M. Venkatesan, C. B. Fitzgerald, J.G. Lunney and J. M. D. Coey, *Phys, RW, Lett*, 93, 177206-177209 (2004).
13. Nguyen Hoa Hong, Antoine Ruyter, W.Prellier, Joe Sakai and Ngo Thu Buong, J.Phys; Condens Matter 17,6533-6538 (2005).
14. J. Dubowik, I. Goscianska, Y. V. Kudryavtsev and A. Szlaferek, *JMMM* 310, 2773-2775 (2007).
15. C. M. Liu, L. M. Fang, X. T. Zu and W. L. Zhou, *Phys. Scn*, 80, 065703 (5pp) (2009).
16. Yuhua xia, Shi hui Ge, Lixi, Xueyunzhou *et al.*, *Applied Surface Science* 254, 7459-7463 (2008).
17. Subhash C. Kashyab, K. Gopinadhan, D. K. Pandya, Subject chandhary, *JMMM* 321, 957-962 (2009).
18. Junying zhang, Quyun, Qianghong wang, *Modern Applied Science*, Vol.4, No.11; (2010).